SPATIO-TEMPORAL ASSESSMENT OF LAND USE AND LAND COVER CHANGES AND THEIR IMPACTS ON LAND SUITABILITY FOR MAIZE PRODUCTION IN FEDERAL UNIVERSITY OF AGRICULTURE ABEOKUTA, OGUN STATE, NIGERIA

TOBORE ANTHONY

Federal University of Agriculture Abeokuta, Abeokuta, Ogun State, Nigeria
Department of Soil Science and Land Management, College of Plant Science and Crop Production.
toboreao@funaab.edu.ng; +2348108840248; anthonytobore@gmail.com; P.M.B. 2240, Abeokuta, Ogun State, Nigeria; Federal University of Agriculture, Abeokuta.

ABSTRACT

The main causes of land-use change are rooted in the spatiotemporal interaction between biophysical and human activities. This study identified the impacts of land use and land cover changes (LULCCs) on land suitability for the years 2000, 2010, and 2020, using Landsat satellite images. Soil samples were collected and analyzed at 0-30 cm soil depth. Principal component analysis and parametric methods were performed on the soil properties to identify suitable areas for maize production. The Markov Chain (MC) and Cellular Automata (CA) methods were utilized to simulate the LULC maps for the year 2030. The accuracy of LULC simulation models is more than 85% based on the validation results. The results of the LULCCs indicated that built-up and farmland increased by 86.99% and 7.07%, and vegetation, grassland and waterbodies decreased by 5.30%, 0.53% and 0.09% respectively. Comparing the results of the three parametric methods used showed that the Rabia equation gave higher suitability index values than the Stories and Square root methods. Multicriteria analysis of the land suitability revealed that most of the study area was marginally not suitable at 6915.4 ha (69.1%), and marginally suitable at 2598.5 ha (26%) while only a very small part of the land was moderately suitable at 298.4 ha (3.0%) and highly suitable 187.8 ha (1.9%) for maize production. The main limiting factors were slope, rainfall, temperature and erosion hazard. Thus, modelling and simulating LULCCs using the CA-Markov model plays a significant role in land use policymaking, planning and ensuring sustainable land suitability.

Keywords: ***Land use, Markov-chain, GIS-parametric, Maize-suitability, Remote sensing***

INTRODUCTION

Land use and land cover changes (LULCCs) are one of the most essential drivers and important interactions between human and global environmental systems (Lambin, 1999). Land use is described as the ways and purpose in which human beings employ the land and its resources (Mwavu and Witkowski, 2008) while land cover refers to the physical appearance and ecological state of the land surface (Alemayehu *et al.,* 2009). One of the driving mechanisms of modelling LULCCs is to analyze the past, and present, and simulate possible future changes (Verburg *et al.,* 2011; Wu *et al.,* 2013). Monitoring and mitigating the negative consequences of LULCCs have become the main driving force of researchers and policymakers around the world (Zhang *et al.,* 2015).

Land suitability analysis is a method of detecting inherent capacities and potential suitability of crops such as maize (FAO, 1976). According to Verheye (2008), most cultivated lands have been degraded and become unsuitable for crop production, especially maize (Foley *et al.,* 2005). Maize is one of the five food crops promoted in the attainment of food self-sufficiency in Nigeria (FAO, 2009). Nevertheless, optimum food self-sufficiency such as maize production can be attained when the land is properly investigated and put into the best use (Senjobi, 2007). Hence, the term "Land suitability" refers to the investigation of a certain part of land's appropriateness to a specific type of land use which can be directly or indirectly controlled by the land ability to produce optimally (Vargahan *et al.*, 2011).

Consequently, traditional techniques for mapping LULCCs are time-consuming, costly and not adequate for multi-complex environmental studies, especially when compared with digital methods (Tobore *et al.*, 2019). In recent years, more attention has been directed towards Remote Sensing (RS) and Geographical Information Systems (GIS) due to their high efficiency and cost-effectiveness for mitigating and monitoring land-use sustainability (Zubair, 2006). Although, modelling and simulating LULCCs and their impact on land suitability for maize production have been investigated and assessed through various methods such as Rabia equation of land suitability evaluation (Rabia, 2012), cellular automata models (Singh *et al.*, 2015), statistical analysis (Vargahan *et al.*, 2011), Markov chain (Mishra *et al.*, (2018) and artificial neural network (Subedi and Thapa, 2013). However, integration of the Rabia equation, cellular automata (CA) and Markov chain (MC) model are becoming widely used because of their bottom-up approach, actual estimation of land potentials and high flexibility efficiency with spatial data (Saaty, 1977; Vargahan *et al.*, 2011; Mustafa, 2011; Rabia, 2012: Subedi *et al.*, 2013; Ansari *et al.*, 2016). Recently, several studies have documented the CA–Markov chain techniques in modelling and simulating LULCCs (Hasan et al. 2017; 2012; Subedi *et al.*, 2013; and Gong *et al.*, 2015). On the other hand, studies on the application of land suitability using the Analytical Hierarchy Process (AHP) have been done through pairwise comparison techniques (Saaty, 1977; Mustafa, 2011; Tobore *et al.*, 2022).

Moreover, with the advancements in geospatial techniques, RS and GIS have provided a better way for monitoring and mapping LULCCs integrated with land suitability assessment at less time, low cost, and with higher accuracy (Wu *et al.*, 2017). The present study emphasized the use of RS and GIS techniques to monitor and map the past, present and more importantly possible future of LULCCs at the Federal University of Agriculture Abeokuta (FUNAAB), Ogun State, Nigeria. The study is targeted to assess the land suitability of the area for maize production using the Rabia index suitability method. Therefore, the objectives of this study were to predict the land use cover changes from the year 2000 to 2030 using the CA-Markov change model and assess the soil nutrients of the study area for maize production.

Materials and Methods

Description of the study area

The study area is located between latitudes 7°13'N and 7°20'N and longitudes 3°20'E and 3°28'E enclosing approximately 10,000 hectares (ha) of land (Fig. 1). The area which is north of Abeokuta city encloses the landmass of the Federal University of Agriculture Abeokuta (FUNAAB) campus. It is characterized by extensively mild slopes bounded into six zones and punctuated in parts by ridges, isolated residual hills and plateaus, and valley landscapes with lowlands (Ufoegbune, *et al.*, 2010).

Climate

The climate of the area is humid tropical type, characterized by a wet and dry season (Adebekun, 1978). The wet season lasts from April to October with an annual rainfall of about 2500 mm at the coast and about 1220 mm at the northern limit of the forest belt. The monthly mean minimum temperature is about 22.48°C while the monthly mean maximum temperature is about 31.24°C with an average yearly temperature of about 26.6°C (Adeleye *et al.,* 2020). Furthermore, the average yearly relative humidity is about 76.05% (Federal Office of Statistics, 1988).

Geology and soils

The geology of the study area overlies metamorphic rocks of the basement complex, the great majority of which are ancient being of pre-Cambrian age. These rocks show great variation in grain size and mineral composition, ranging from very coarse grain pegmatite to fine-grained schist and from acid quartzite to basic rocks consisting largely of amphibolite (Smyth and Montgomery, 1962). The soils support the development of the lowland rainforest (Ekanade, 2007). Table (1) shows the classified soil types used in line with the easy assessment of the LULCCs of the study.

Study Methods

Data acquisition and description

Both primary and secondary data were used for this study. The fieldwork started with a reconnaissance visit to the study area, followed by primary data collection. During the reconnaissance survey, ground-truthing information was acquired to define the nature of the ground covers. Field samples from each land use type were collected using Garmin handheld Global Positioning System (GPS) device. Secondary data, spatial and written information such as, base maps including roads, rivers and digital elevation models were acquired through downloading from the United States Geological Survey (USGS) repositories websites. For the present study, Landsat 7 Thematic Mapper (TM) imagery for the year 2000 and 2 sets of Landsat 8 Operational Land Imager (OLI) satellite images for the years 2010 and 2020 were acquired and used to assess the LULCCs. To avoid atmospheric error and seasonal variation, the Landsat images were downloaded during the dry season. Since the Landsat satellite images are free of radiometric and geometric distortions, there was no additional geo-rectification or image-to-image registration needed for image pre-processing. Information on the images acquired from the USGS online data repository is shown in Table (2).

Multi-temporal land cover mapping

The collected satellite images were enhanced in the Idrisi Selva Software environment via (3 by 3) majority filter techniques for better visibility. True Color Composite (TCC) was generated using suitable combinations of bands for the images (d'Entremont and Thomason, 1987; Hussain 2018). Considering the "Nigeria land use classification System" and the goal of this study, Anderson *et al.*, (1976) land use classification scheme II and prior knowledge of the study area for over six (6) years was used to identify the Area of interest (AOI) features. The images obtained from the Landsat image were classified into 5 land use and land cover (LULC) classes based on the Maximum Likelihood Supervised Classification (MLSC) algorithm techniques (Table 3). The MLCS operation is carried out due to its good performance and easy classification algorithm (Liu, 2005; Sun *et al.,* 2013; Biro *et al.,* 2013; Zhang *et al.,* 2015). The accuracies of land cover maps were evaluated through 150 ground truths from field data and with the support of the year 2020 Google Earth image. These 150 pixels were chosen through the random sampling process. The Kappa statistics and confusion matrix was calculated for accuracy assessment (Story and Congalton, 1986; Foody, 2002; Pontius Jr and Millones, 2011).

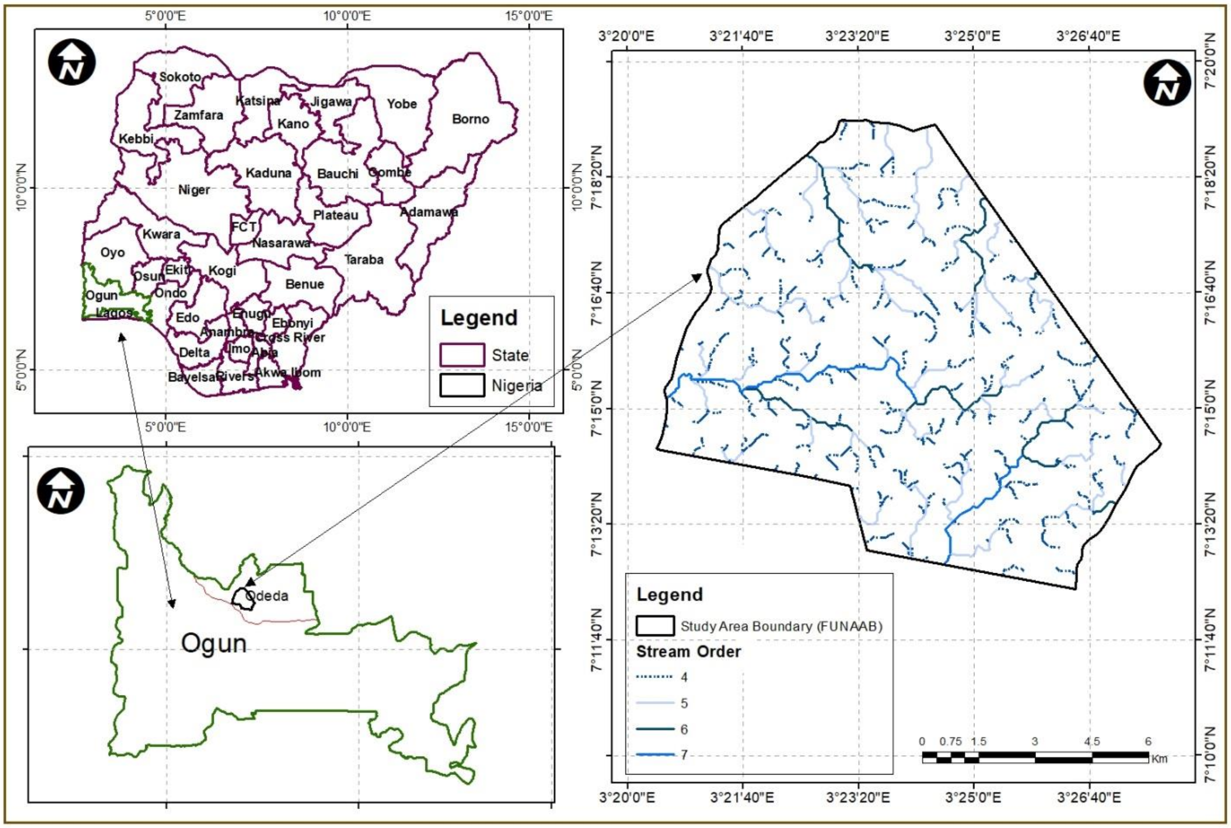

Figure 1: A map showing the Federal University of Agriculture, Abeokuta

Table 1: USDA-FAO/UNESCO classification and description of the FUNAAB soils

Soil Series	USDA	FAO/ UNESCO	Soil Description
Apomu	Oxic Paleustalf	Ferric Luvisols	Derived from colluvial materials: Occupy moderate to gentle slopes; very sandy to a depth of ≥ 50 cm; free of stones and concretions
Egbeda	Rhodic Paleustalf	Ferric Lixisols	Occupy level to gentle slopes; bright orange to brownish red between 25 and 120 cm depth.
Ekiti	Lithic Troporthent	Lithosols	Skeletal in nature and of comparatively recent origin: occurrence is limited to small patches close to exposed rock surfaces usually on hill or crest summits
Iseyin	Oxic Ustopept	Ferric Cambisols	Hill creep soils: pale grayish brown to dark reddish-brown: sandy clay to clay.
Iwo	Kandic Paleustalf	Ferric Lixisols	Occupy level or gentle slopes: profile is grayish brown to brownish red; fairly clayey within 50cm; a sand fraction is usually coarse and small fragments of feldspar are often present.
Jago	Typic Tropaqualf	Gleyic Luvisols	Occupy gentle to level slopes; usually close to temporary to perennial streams; pale grayish brown to pale yellowish-brown and yellow colour being common.
Okemesi	Oxic Tropudalf	Ferric Luvisols	Occupy steeply sloping sandy; not heavier than clayey sand on the horizons above 40 – 50 cm usually shallow

Source**:** Sotona *et al.*, (2013).

Table 2: Landsat satellite images characteristics used for the study

Satellite Image	Acquisition date	Path and row	Used bands composite	No of bands	Scale/Resolution	Source
LandSat 7TM	06/01/2000	P191, R55	432	5	30m by 30m	USGS
LandSat 8OLI-TIRs	19/01/2010	P191, R55	652	10	30m by 30m	USGS
LandSat 8OLI-TIRs	20/01/2020	P191, R55	652	11	30m by 30m	USGS

Table 3: Description of land use and land cover categories

No	Class name	Description
1	Built-up	Lecture hall, offices and laboratories
2	Vegetation	Mixed forest and grass
3	Bare land	Vacant land, open space, sand, bare soils and landfill sites
4	Farmland/Grassland	Fallow land Rainfed cropping planted cropping areas.
5	Waterbodies	River, exposed water bodies, ponds, dams, creeks and streams.

Modelling and simulation pattern analysis

Firstly, three calibration periods, i.e. 2000-2010, 2010 - 2020, and 2000 - 2020 were considered and correspondent simulation results were pre-analyzed in terms of goodness of fit. To simulate the future LULC pattern of the study area, the Markov chain (MC) and cellular automata (CA) model methods were applied. Markov chain performs better at modelling LULC in both temporal and spatial dimensions for its higher accuracy (Pontius Jr and Millones, 2011). A cellular automata underlies the dynamics of LULC change for any location (cells) based on the concept of proximity (Balogun and Ishola, 2017). To simulate LULCCs of the study area, the CA-Markov model was implemented in the LandSat images through the Idrisi Selva environment. The LULC change prediction was based on the dependent and independent variables. The dependent variables used are the digital elevation model (DEM), aspect, slope and distance from the major road (Figures 2 and 3). The DEM, slope and aspect were produced from ASTER of 30-meter raster resolution downloaded from the USGS website. The DEM and aspect range from the lowest value of -16 meters to the highest value of 287 meters from mean sea level (MSL), the slope was classified as flat to very steep according to FAO (1990). The distance from a major road was derived from vector layers from an open street map. Analysis of the distance from major roads was carried out with a geoprocessing tool using Euclidean Distance (EU) in Arc-Map 10.5 environment. The results of the analysis were extracted by the mask to clip the study area from the open street map. Thereafter, the vector layers were reclassified based on the shortest distance of the study area. The independent variables are the LULC of the years 2000, 2010 and 2020 classification maps of the study area. The independent and dependent variables were used as input parameters to generate the transition probability matrix in the IDrisi Selva environment. The transition matrix analysis generates an empirical likelihood image that estimated the probability of change between LULC of the study area. The random sampling method was applied using the maximum iteration and neighborhood of 3 by 3 i.e. 9 cells. The CA-Markov were predicted according to Ma *et al.* (2012) and expressed as:

$S_{t+1} = P_{iJ} \times S_{t}$…………………. …… 1

Where: S is the land-use status

t+1 is the time point

P_{iJ} is the state transition probability matrix

$$P_{iJ}\begin{bmatrix} P_{11}, & P_{1}, & P_{1}, \\ \cdots, & \cdots & \cdots \\ P_{11} & P_{11} & P_{11} \end{bmatrix}\text{…………..…… 2}$$

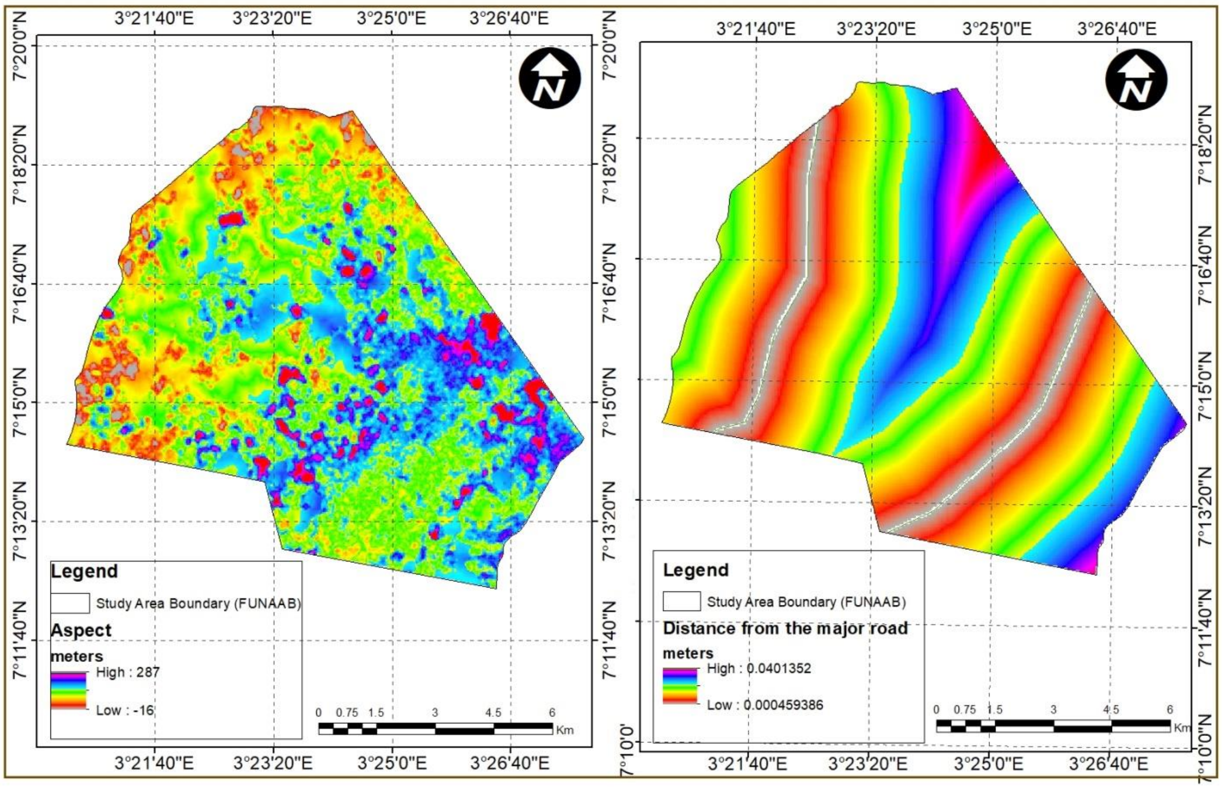

Figure 2: Aspect and distance from the major road of the Federal University of Agriculture, Abeokuta

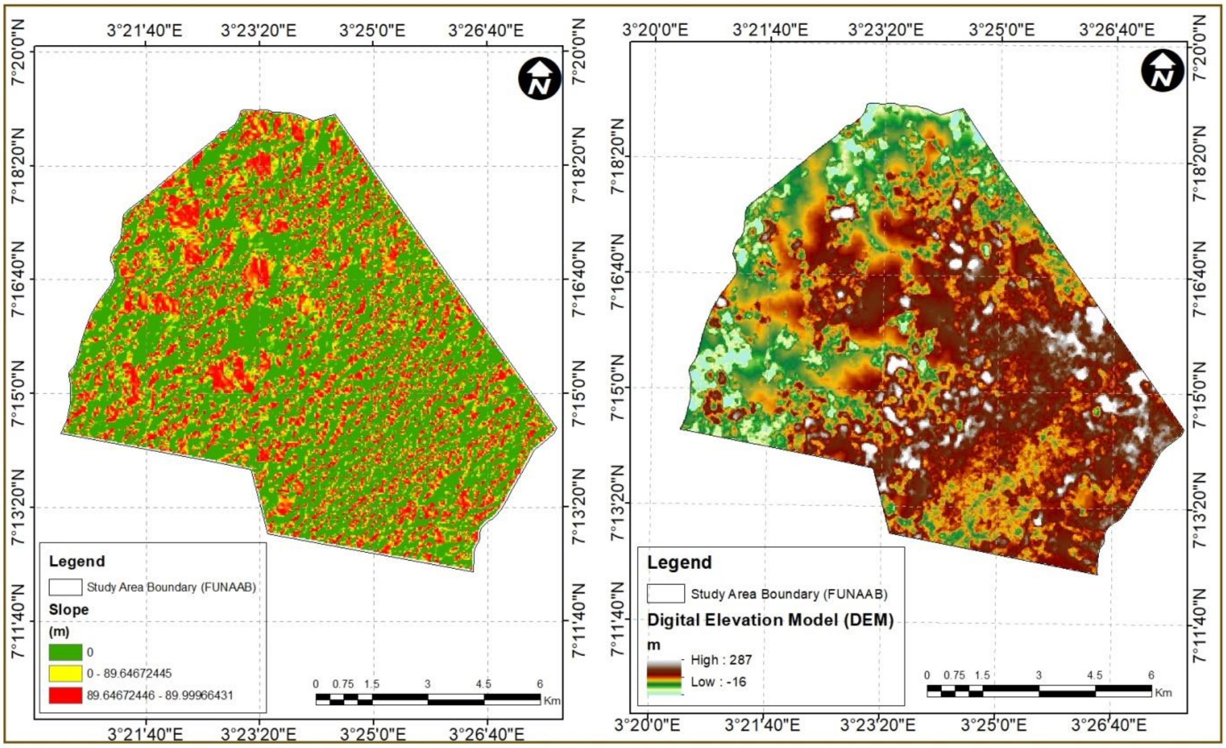

Figure 3: Slope and digital elevation model of the Federal University of Agriculture, Abeokuta

Accuracy assessment

Accuracy assessment is the process of generating a set of points from the classified image by the ground truth data from the original maps (Liu, 2005). In this study, to ensure the model acceptance in predicting LULC change for the projected year, a validation process was performed using the existing database. The CA-Markov model was validated to simulate LULC of the year 2020, which was compared to the estimated LULC map of the same year. The validation process was performed in the IDrisi selva software environment and the Kappa (K) parameters were obtained (Cohen, 1960; Pontius Jr and Millones, 2011). Kappa parameters are tests used to measure the accuracy between predefined producer rating and user-assigned rating (Pontius Jr and Millones, 2011). The Kappa test can be expressed as:

$$K = \frac{\mathrm{P\ (A) - P\ (E)}}{1 - \mathrm{P\ (E)}} \ldots\ldots\ldots\ldots..\ldots\ldots\ldots\ldots\ 3$$

Where:

$P\ (A)$: the number of times the k raters agree,

$P\ (E)$: the number of times the k raters are expected to agree only by chance.

Criteria for land suitability analysis

Vegetation cover analysis

Table (4) shows the land suitability criteria assessment used for the study. Vegetation indices derived from satellite remote sensing data are one of the primary sources of information for monitoring the Earth's vegetation cover (Gilabert *et al.*, 2002). Normalized difference vegetation index (NDVI) is a traditional vegetation index that is correlated with several important biophysical properties applied to generate different crop indices (Ahamed *et al.*, 2016). In contrast, the Soil-adjusted vegetation index (SAVI) is a modification of NDVI that corrects the influence of soil brightness when the vegetation cover is low (Jiang *et al.*, 2006). In this study, the NDVI data were used to calculate the Proportion of Vegetation (PV) of the study area for the years 2000, 2010 and 2020. SAVI was also used to reduce the soil background effect using the soil adjustment factor L for the same years. The NDVI and SAVI were calculated using temporal information from Landsat 7 for the year 2000 and Landsat 8 OLI image datasets for the years 2010 and 2020 (Figures 4 and 5). Huete (1988) described NDVI and SAVI as follows:

$$NDVI = \frac{\mathrm{NIR} - \mathrm{RED}}{\mathrm{NIR} + \mathrm{RED}} \ldots\ldots\ldots\ldots\ldots\ldots\ldots\ldots\ldots \; 4$$

Where:
NIR is the Near-infrared (NIR) region of band 5
RED is the visible red of band 4.

$$SAVI = \frac{(\mathrm{NIR} - \mathrm{RED})}{\mathrm{NIR} + \mathrm{RED} + \mathrm{L}} \ldots\ldots\ldots\ldots\ldots\ldots\ldots \; 5$$

Where:
NIR is the near-infrared regions of band 5,
Red is the visible red of band 4, and
L is the constant or correction factor, ranging from 0 to 1.

Land surface temperature (LST)

Accurate land surface temperature (LST) retrieval from remote sensing data depends on emissivity and geometry (Gao *et al.*, 2013) For this study, LST was calculated using temporal information from the Landsat images for the years 2000, 2010 and 2020 (Figure 6). For the estimation of the year 2000 LST, Landsat 7 TM image was used and subjected to two-step procedures. Step 1: This was carried out by converting the digital numbers (DNs) of band 6 to radiation luminance (Li *et al.*, 2004) by the equations (6) – (7).

$$R_{TM6} = \frac{V}{255} (\mathrm{R_{max}} - \mathrm{R_{min}}) + \mathrm{R_{min}} \ldots\ldots\ldots 6$$

Where: R_{TM6} represents radiation luminance V represents DN of band 6 and

$\mathrm{R_{max}} = 1.896\ (\mathrm{mW} * \mathrm{cm}^{-2} * \mathrm{sr}^{-1})$……. 6.

$\mathrm{R_{min}} = 1.896\ (\mathrm{mW} * \mathrm{cm}^{-2} * \mathrm{sr}^{-1})$…….. 7.

Step 2: The R_{TM6} (radiation luminance) was further converted to LST in Kelvin by equation (8) and thereafter converted to Celsius using equation (9):

$$T_{\mathrm{k}} = \frac{K_1}{ln\left\{\frac{K_2}{\mathrm{RTM6}/\mathrm{b}}\right\}+1} \ldots\ldots\ldots\ldots\ldots\ldots\ldots\ldots.. 8.$$

Where: K_1: $(constant) = 1260.56$
K^2: $607.66\ (\mathrm{mW} * \mathrm{cm}^{-2} * \mathrm{sr}^{-1}\ \mu\mathrm{m}^{-1})$; and
b: (spectral range) = 1.239 (µm).

$$T^0 c = T_{\mathrm{k}} - 273 \ldots\ldots\ldots\ldots\ldots\ldots\ldots\ldots\ldots 9.$$

To estimate the LST for the year 2010 and 2020, Landsat 8 OLI thermal bands were used. Two steps were also followed to derive the LST of the study area from equations (10) – (15).

Step 1: The NDVI data derived were used to calculate the PV which can be expressed as follows:

$$PV = \left(\frac{\mathrm{NDVI} - \mathrm{NDVI_{min}}}{\mathrm{NDVI_{max}} - \mathrm{NDVI_{min}}}\right)^2 \ldots\ldots\ldots\ldots\ldots\ldots \; 10$$

Where:
PV: is the proportion vegetation
$\mathrm{NDVI_{min}}$, was retrieved from the NDVI minimum value, which is -1, and
$\mathrm{NDVI_{max}}$, retrieved from the NDVI maximum value, which is 1. Hence, the PV was further expressed as follows:

$$PV = \left(\frac{\mathrm{NDVI}+1}{2}\right)^2 \ldots\ldots\ldots\ldots\ldots\ldots\ldots\ldots\ldots 11.$$

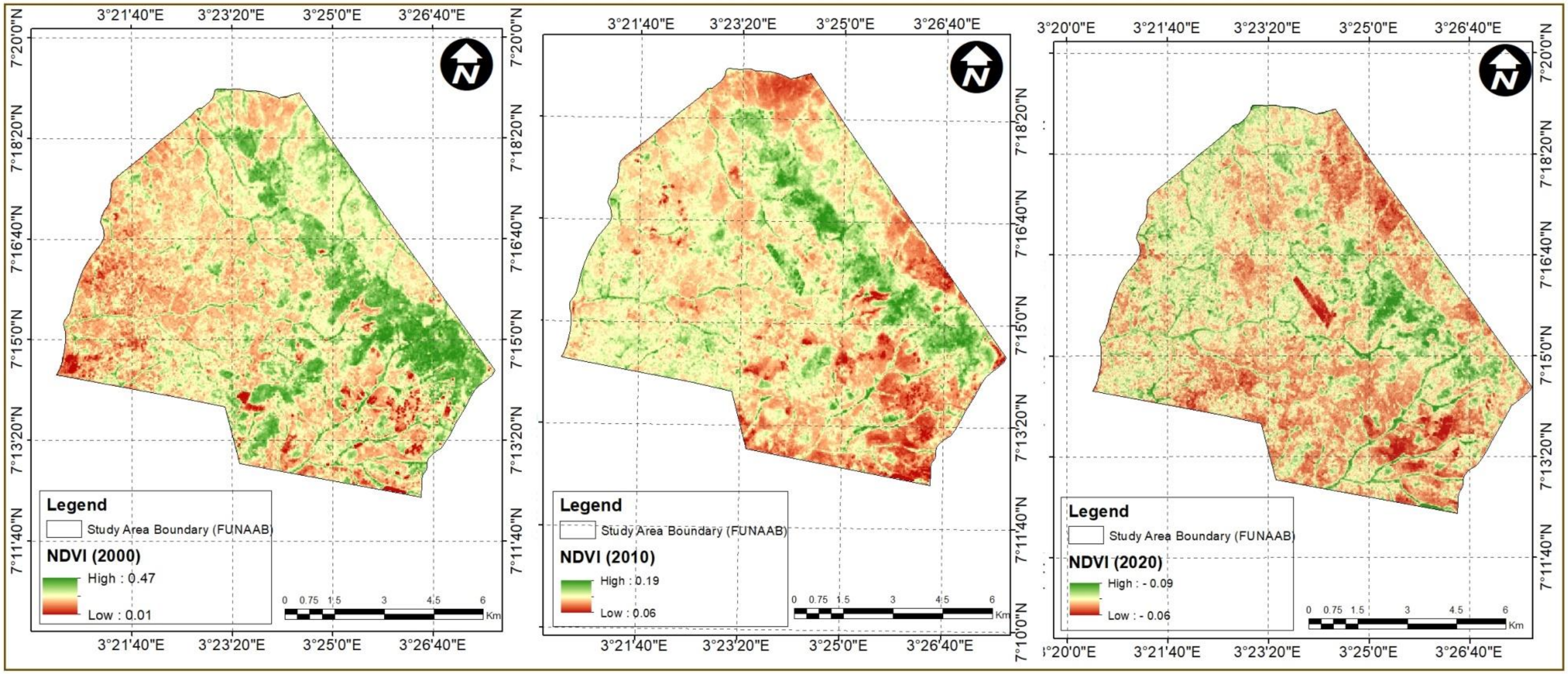

Figure 4: Normalized Difference Vegetation Index (NDVI) of the Federal University of Agriculture, Abeokuta

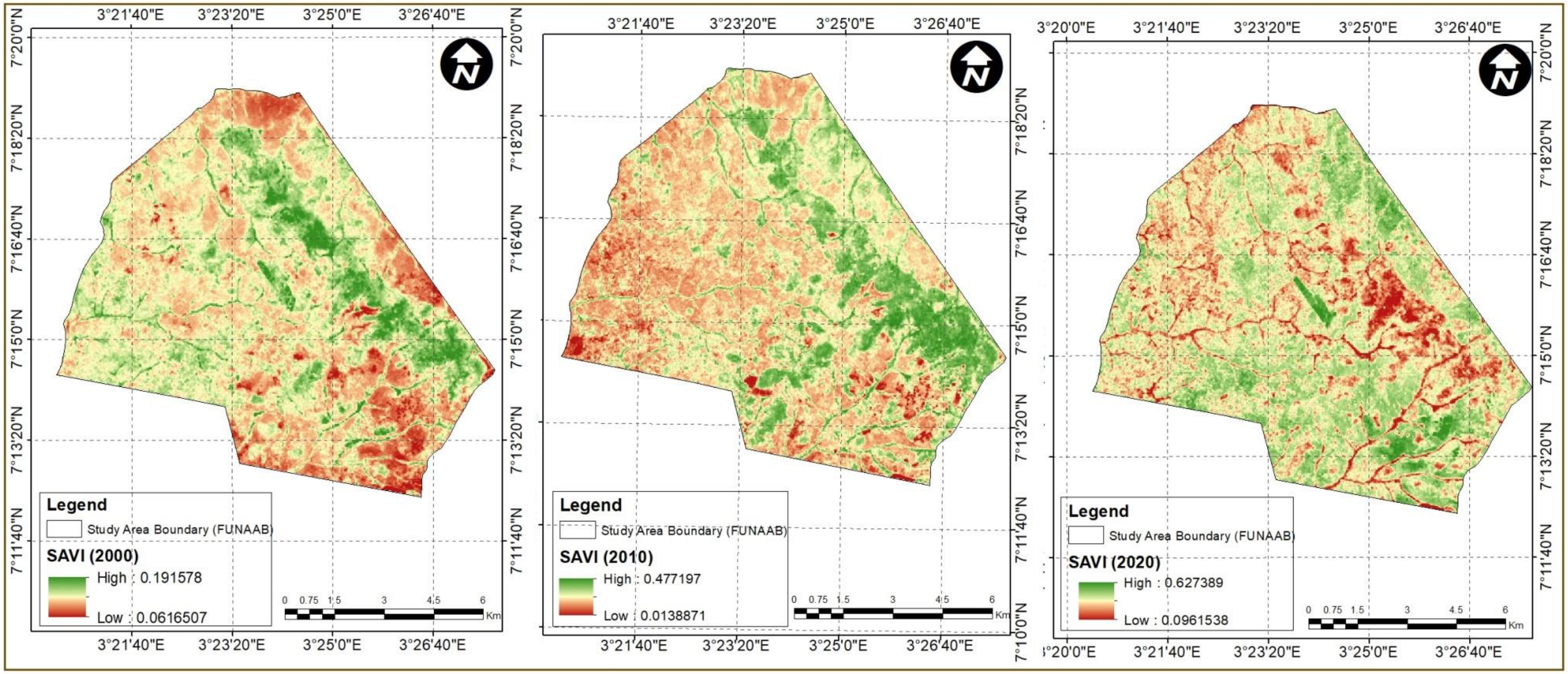

Figure 5: Soil Adjusted Vegetation Index (SAVI) of the Federal University of Agriculture, Abeokuta

Step 2**:** The thermal bands were converted to DNs to estimate the spectral radiance of the study area using bands 10 and 11 in the Landsat 8 OLI image (Rasul *et al.*, 2015). The spectral radiance was described below and subjected to equation (12):

$L\lambda$= 0.0003342* Band10 +0.1 and $L\lambda$= 0.0003342* Band11 +0.1). … … … … … … … … … … … … … … … 12.

$L\lambda = ML + Q_{CAL} + AL$

Where:

$L\lambda$ *is the spectral radiance at the sensors aperture*

ML is the band-specific multiplicative rescaling factor from the metadata,

Q_{CAL} is the quantized and calibrated standard product pixel (digital number) values,

AL is the band-specific additive rescaling factor from the metadata.

Thereafter, the Land Surface Emissivity (LSE) and Brightness Temperature (BT) of the study area were calculated and described according to Jesus and Santana (2017) using equations (13) and (14):

$$LSE = 0.004 * PV + 0.986 \ldots\ldots\ldots\ldots\ldots 13$$

Where: LSE is the land surface emissivity of the study area

PV: is the proportion of vegetation of the study area; and

$$BT = \frac{K2}{ln\left\{\frac{K1}{L\lambda}\right\}+1} - 273.15 \ldots\ldots\ldots 14$$

Where: BT is the satellite brightness temperature (Celsius)

K2 is the calibration constant 2 (Kelvin), thermal conversion constant from the metadata;

K1 is the calibration constant 1 (Kelvin), thermal conversion constant from the metadata;

Therefore, the LST of the study area were further calculated using equation (15) and expressed according to Jesus and Santana (2017):

$$\text{LST} = \frac{BT}{1\left(\frac{\lambda BT}{PV} * \ln LSE\right)} \ldots\ldots\ldots\ldots\ldots 15$$

Climatic analysis

Climatic data are one of the most important land characteristics to be considered when optimum rainfed maize potential is desired (Epule *et al.*, 2017). The remotely sensed daily climatic data namely; minimum and maximum temperature and rainfall for the study region were obtained from https://power.larc.nasa.gov/ for the year 1983 – 2019. The rainfall and temperature data collected were then processed according to the mean annual data. Thereafter, the mean annual rainfall and temperature were presented as bar and line graph using R-statistics (Figure 7).

Soil mapping and analysis

Reconnaissance and stratified random sampling were applied based on the soil survey manual (FAO, 2007a). Soil samples were collected at the soil depth of 0 – 30 cm for soil analysis with the aid of soil auger. Thereafter, the entire soil auger observations points were georeferenced with the help of handheld GPS to assess the soil nutrients distribution of the study area. On the other hand, coordinates of the soil samples depth were taken using handheld GPS for easy and accurate mapping of the study area. At each soil types, 4 representative soil samples were collected at a 200-meters interval and clustered together to make a total of 28 soil samples. Thereafter, the soil samples were prepared in the laboratory after air-drying at room temperature for soil analysis. Coordinates of physiographic features were taken with the aid of a GPS and properly documented for land suitability mapping analysis for maize production using ArcGIS 10.5 software environment. The soil properties were subjected to FAO (1976) land suitability evaluation following the procedure described by Sys *et al.*, (1991).

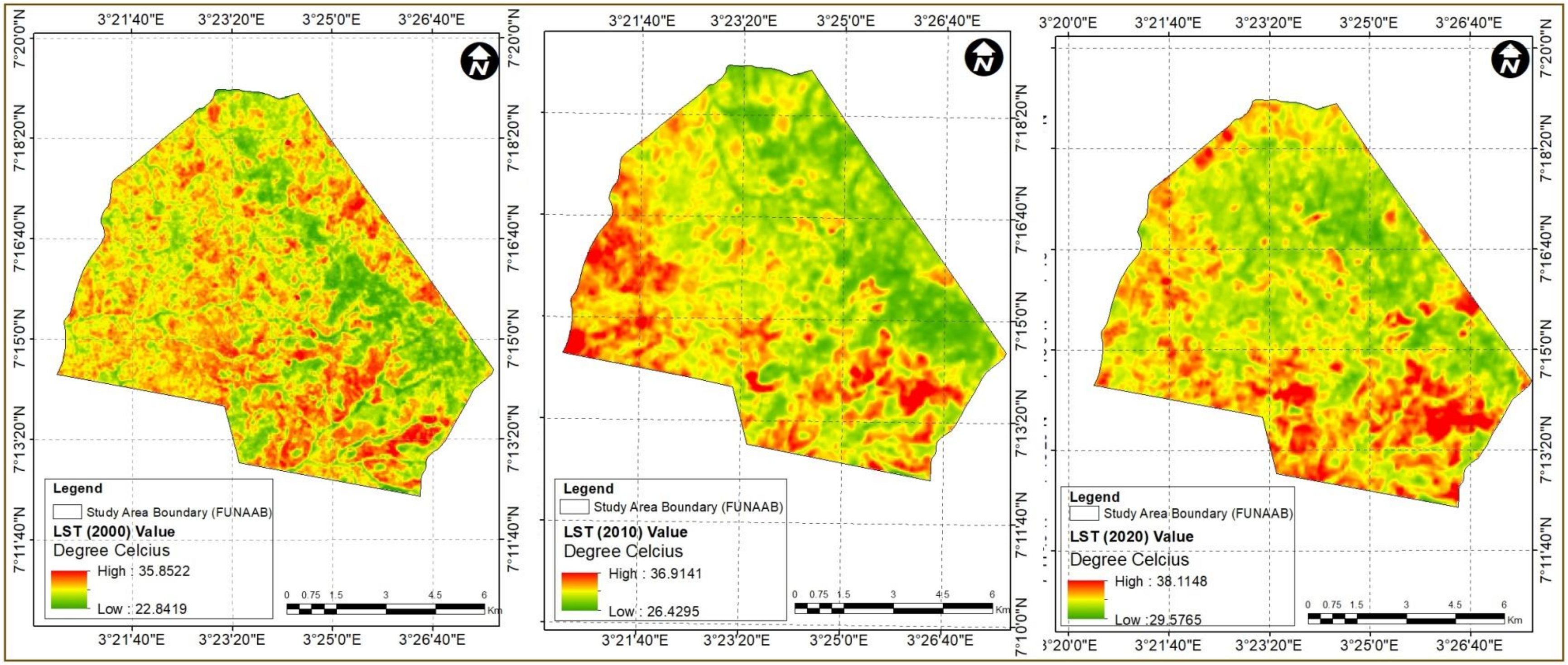

Figure 6: Land Surface Temperature (LST) of the Federal University of Agriculture, Abeokuta

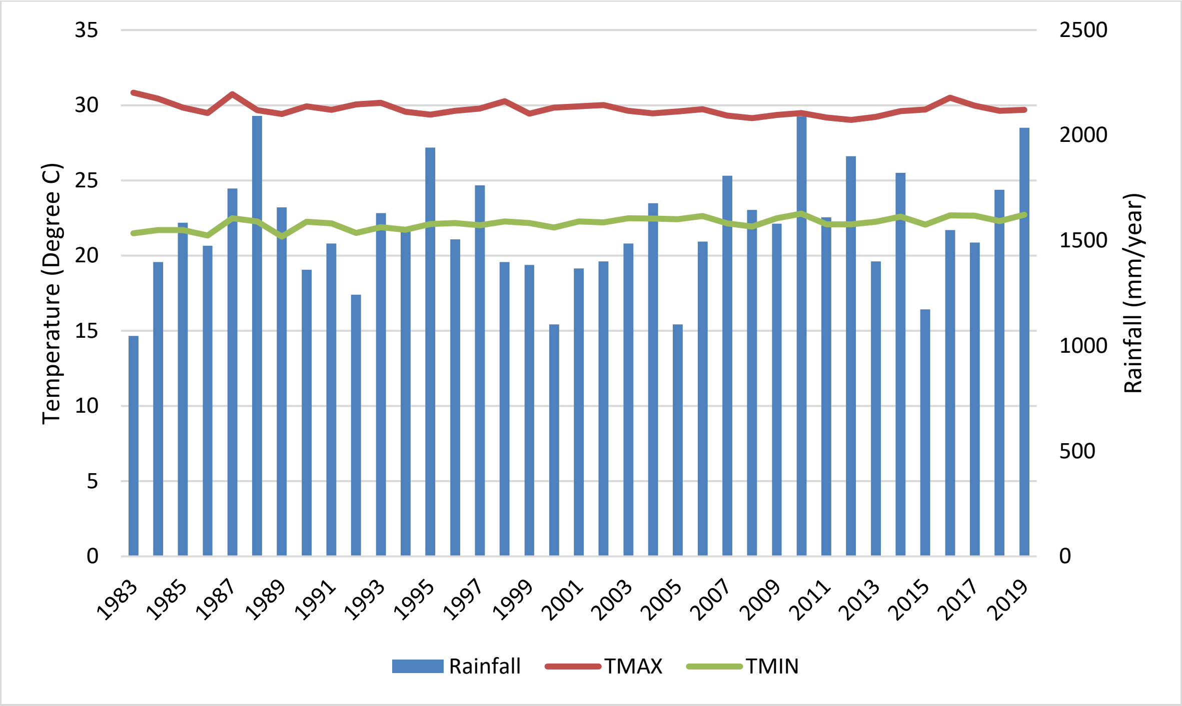

Figure 7: Rainfall and Maximum and Minimum temperature of the study area

Table 4: Criteria for land suitability analysis used for the study

No	Land Criteria	Sources	Acquisition
1	NDVI	USGS Landsat 7 and Landsat 8	2000, 2010 and 2020
2	SAVI	USGS Landsat 7 and Landsat 8	2000, 2010 and 2020
3	LST	USGS Landsat 7 and Landsat 8	2000, 2010 and 2020
4	Rainfall	https://power.larc.nasa.gov/	1983 – 2019
5	DEM/Slope	ASTER	2019
6	LULC	USGS Landsat 7 and Landsat 8	2000, 2010 and 2020
7	Soil Analysis	FUNAAB	2019

Laboratory data analyses

The soil samples were air-dried and passed through a 2 mm sieve before analysis for their physical and chemical properties. The particle size distribution of the soil was determined by the hydrometer method (Bouyoucos, 1962).

Soil pH was determined in 1:2 water suspensions with a glass electrode pH meter (McLean *et al.*, 1982). Soil organic carbon was determined by the chromic acid oxidation method (Walkley and Black, 1939). The total nitrogen of the soil was determined by the micro Kjeldahl method (IITA, 1988). The soil available phosphorus was determined according to the Bray-1 method (Nelson and Sommers, 1996). The Exchangeable bases (Ca^{2+}, Mg^{2+}, $K^{+,}$ and Na^{+}) in the soil were extracted with 1 N ammonium acetate solution. For heavy metal analyses, sub-samples (0.5 g) of each of the soil sample were digested. Digestion was done with 10 ml of a mixture of nitric (HNO^{3}) and perchloric ($HClO^{4}$) acid in ratio 2:1 (v/v) for 90 min, initially at 150°C., after which 2 ml of concentrated Hydrochloric Acid (HCl) was added to the mixture. The temperature of the digest was then increased to 230° C for another 30 minutes on the digester. On completion of digestion, the digests were allowed to cool at room temperature. Thereafter, the content of each digestion tube was transferred into a 50 ml volumetric flask and made to volume with distilled water, afterwards, the content of each digestion tube was transferred into a 50 ml volumetric flask, made to volume with distilled water and read through atomic absorption spectrophotometer (Das and Ting, 2017).

Land suitability assessment

The parametric approach was used to assess the land suitability of the study area using the Rabia equation of land suitability evaluation. Rabia's equation of land suitability is a parametric evaluation that compares the Storie and Square root methods in a study (Rabia, 2012). The parametric approach was subjected to 0 – 30 cm of soil depth for land suitability analysis of the study area. Storie, Square root, and Rabia equation of land suitability evaluation methods can be expressed in the formula as:

Storie method:

$$S_{\mathrm{i}} = A \times \frac{B}{100} \times \frac{C}{100} \times \frac{D}{100} \times \ldots\ldots\ldots.\ldots \quad 16$$

Where, S_{i} = suitability index

A = rating value for soil texture and

B, C, D = rating values for other parameters.

Square root method:

$$S_{\mathrm{i}} = R_{\min} \times \sqrt{\frac{A}{100} \times \frac{B}{100} \times \frac{C}{100} \times} \ldots\ldots\ldots \quad 17$$

Where, S_{i} = suitability index

$R_{\min}$ = is the minimum rating value of the parameters,

A, B, C, = the remaining rating values for other parameters.

Rabia method:

$$S_{\mathrm{i}} = W_{\max} \times \sqrt{\frac{A}{100} \times \frac{B}{100} \times \frac{C}{100} \times} \ldots\ldots 18$$

Where

S_{i} = suitability index

$W_{\max}$ = is the rating value of the parameters that has maximum weight,

A, B, C, = the remaining rating values for other parameters

Multicriteria assessment

Land suitability evaluation for optimum rainfed maize production requires some criteria (see Table 3). The collected soil samples of 0 – 30 cm soil depth were used to assess the land suitability evaluation of the study area. Thereafter, the Analytical Hierarchy Process (AHP) described by Saaty and Vargas, (2001) was used to assign weights (values) for the soil properties ranging from 1 to 9 (Table 5). The AHP compares different parameters to each other and gives values of weights according to their relative importance (Saaty and Vargas, 2001; Tobore *et al.*, 2022). Land suitability evaluation rating index and land requirements suitability classes for rainfed maize production were used to assess maize suitability classes to the study soils coupled with AHP using Multi-Criteria Evaluation (MCE) in ArcGIS 10.6 software environment (Tables 6 and 7). The FAO (1976) land suitability evaluation following the procedure described by Sys *et al.*, (1991) was used to assess the maize suitability of the study area. The Sys *et al.*, (1991) can be expressed in the formula:

$$S = f\ (x_1, x_2, \ldots\ldots.., x_n) \ldots\ldots\ldots\ldots\ldots\ldots\ldots 19$$

Where:

S = is the suitability level

x_1, x_2 = are the factors affecting land suitability.

Statistical analysis

The relationship across the soil nutrients was subjected to principal component analysis (PCA) using R- statistics. PCA was used as a valuable method to define the most significant and important soil properties in the differentiation of LULC types within the study area.

Table 5: Preference scale from AHP Pairwise Comparison

Scale	Degree of Preference	Details
1	Equal importance	Two activities contribute equally to the objective
3	Moderate importance	Experience and judgment slightly favour one activity over another
5	Strong importance	Experience and judgment strongly favour one activity over another
7	Very strong importance	An activity is favoured very strongly over another
9	Extreme importance	The evidence favouring one activity over another is of the highest possible order of affirmation
2,4,6,8	Intermediate values between two adjacent judgments	When terms are needed

Source: Saaty and Vargas 2001

Table 6: Land suitability class description and the corresponding suitability index

Suitability Class	Suitability	Suitability index (SI)	Description
S1:	Highly suitable	> 75	Land without any significant limitation
S2	Moderately suitable	50 – 75	A moderately severe limitation which reduces productivity
S3	Marginally suitable	25 – 50	Overall severe limitations; given land use is only marginally justifiable
N1	Marginally not suitable	10 – 25	The land-use type under analysis is not acceptable at all for the land
N2	Permanently unsuitable	< 10	The land-use type under analysis is permanently not acceptable at all for the land

Source: FAO, 2007

Table 7: Land requirements and suitability classes for rainfed maize production

Land characteristics	**SI1** **100**	**SI2** **95**	**S2** **85**	**S3** **60**	**N1** **40**	**N2** **25**
Topography (t)						
Slope (%)	0-2	2-4	4-8	8-16	16-20	>20
Climate						
Total rainfall during the growing season (mm)	800-1200	700-800	600-700	500-600	<500	-
Temperature (°C)	>25	22-25	20-22	18-20	16-18	<16
Oxygen availability (w)						
Drainage	Good	Moderate	imperfect/rapid	poor/very excess	poor but drainable	poor but not drainable
Nutrient availability (0-20cm) (f)						
Total N (%)	>0.15	0.08-0.15	0.08-0.04	0.02-0.04	<0.02	any less
Avail P (mg/kg)	>22	13-22	6-13	3-6	<3	any less
Potassium (cmol/kg $^{-1}$)	>0.5	0.3-0.5	0.2-0.3	0.1-0.2	<0.1	Any
Nutrient retention (n)						
CEC (Cmol/kg -1)	>15	10-15	5-10	3-5	<3	-
Base saturation						
(%)	>80	30-50	35-50	20-50	<20	-
(%)	>70	50-70	35-70	<35	-	-
Organic matter						
(g/kg)	>4	3 - 4	2-3	1- 2	<1	-
Physical soil characteristics						
Texture/structure	CL	SC, SCL, L	SL, LS	LS, S	S,	-
Gravel						
(%)	<15	15-40	40-60	60-75	75-90	>90
(%)	<40	40-75	75-80	80-90	>90	-
(%)	<20	20-40	40-75	>75	-	-
Soil depth (cm)	>90	50-90	30-50	20-30	10-20	<10
Bulk density (g/cm^3)	<1.0	1.0-1.21	1.22-1.51	1.51-1.63	1.63-2	>2

Source: Oluwatosin and Ogunkunle (1991). L = Loamy; SC= Sandy clay; LS =Loamy sand; S = sand; SCL =Sandy Clay Loam, SL =Sandy loam, CL= Clay loam, S=Sandy

RESULTS AND DISCUSSION

Land use and land cover assessment

The output images from the LULC analysis are presented in Figure 8. In the present study, the MLSC algorithm was applied to the Landsat satellite images for the years 2000, 2010 and 2020 focusing on built-up, vegetation, waterbodies, farmland and grassland using the IDrisi Selva software. The CA-Markov model was subjected to visual interpretation, cognition of colours, and patterns which show great efficiency in simulating the year 2030 land use and land cover map of the study area (Figure 9). Bakx *et al.* (2019) posit that one of the intuitive ways of extracting information from remotely sensed images is by cognition of patterns and colours with visual image interpretation. Overall classification accuracy of MLSC was 92.10%, 93.51%, 95.87% and 96.34% in the years 2000, 2010, 2020 and 2030, respectively (Table 8). Based on the evaluation of predicted LULCCs with observed LULCCs scenarios, a Kappa index value was derived. After the prediction, it was found that all Kappa index values were greater than 0.85 showing substantial agreement between predicted and observed LULCCs maps. According to Lu *et al.* (2005) Kappa coefficient is the most common accuracy assessment used in assessing LULC change in a study. The change statistics analysis of the images in each LULC class were estimated and presented in Table 9. The results revealed that built up are the dominant land-use type, covered 1049.8 ha of the study area in the year 2000, 5066.4 ha in the year 2010, and 7909.1 ha in the year 2020. In contrast, vegetation and grassland covered 60.2% and 24.2% of the study area in the year 2000, 24.5% and 2.2% in the year 2010, and 9.3% and 1.5% in the year 2020, respectively. The decrease in vegetation and grassland may have translated into an increase in the waterbodies and farmland in the studied area. The analysis shows that the proportion of waterbodies in the years 2000, 2010 and 2020 was 0.05%, 0.07% and 0.08% in the studied area. However, farmland was 499.9 ha in the year 2000 and decreased from 2247.3 ha to 999.3 ha in the year 2020. The substantial increase in the built up area could be a result of a gradual increase in student populations leading to gradual to sudden increase in human activities in the area. Nevertheless, Lambin *et al.* (2003) stated that increase in the human population and global climate change can be responsible for vegetation cover loss especially in a derived savanna such as the study site (Lepers *et al.*, 2005). The present study is in tandem with Sotona *et al.* (2013) who stated that vegetation cover in FUNAAB was confined into a pocket or fragmented mosaics. Further studies supporting the present study can be found in Victorino (2011).

Table 8: Accuracy assessment of the LULC classified maps for the years 2000 to 2030

	User Accuracy (%)						Producer Accuracy (%)					
LULC	WB	VG	FL	BU	GL	Overall Classified Accuracy (%)	WB	VG	FL	BU	GL	Overall Statistic Kappa
2000	93.3	91.5	93.0	91.3	96.3	92.10	92.4	93.2	93.4	95.1	91.9	0.8878
2010	97.4	94.4	92.4	93.4	97.4	93.51	95.8	94.3	93.9	96.3	92.3	0.8973
2020	98.4	97.4	98.2	96.4	98.4	95.87	96.9	97.8	95.5	97.3	95.5	0.9365
2030	95.9	96.4	97.3	95.3	97.3	96.34	95.8	97.7	94.5	96.4	97.3	0.9335

LULC: WB: Waterbodies; VG: Vegetation; FL: Farmland; BU: Built-up; Grassland

Table 9: Change analysis of LULC from 2000 to 2030

LULC Type	Area in 2000		Area in 2010		Area in 2020		Area in 2030	
	(ha)	%	(ha)	%	(ha)	%	(ha)	%
Builtup	1049.8	10.49	5066.4	50.66	7909.1	79.08	8700.2	86.99
Vegetation	6023.9	60.23	2456.3	24.56	930.3	9.30	530.3	5.30
Waterbodies	5.9	0.05	7.1	0.07	8.3	0.08	9.3	0.09
Farmland	499.9	4.99	2247.3	22.47	999.4	9.99	707.3	7.07
Grassland	2420.8	24.2	223.2	2.23	153.3	1.53	53.2	0.53
Total	10000.3	100	10000.3	100	10000.3	100	10000.3	100

Multi-temporal land cover transition assessment

The analysis of the magnitude of changes in the study area was assessed for the periods of years i.e. 2000-2010, 2010-2020, 2000-2020 and 2020–2030. A negative sign indicates losses of the LULC change in the study area (Table 10). The study shows that the area has undergone very significant changes focusing on built up, vegetation, bareland, farmland and waterbodies. The present study in tandem with the study of Su *et al.* (2012) and Zheng *et al.* (2015) who noted that simulating LULC change is one of the important global changes predicted for the future especially, in developing countries like Nigeria.

Table 10: Change analysis of LULC changes from 2000 to 2030

LULC Type	**The annual rate of change**							
	2000-2010		2010-2020		2000 – 2020		2020-2030	
	(ha)	%	(ha)	%	(ha)	%	(ha)	%
Builtup	4016.6	30.2	2842.7	36.2	6859.3	40.3	791.1	40.9
Vegetation	- 3567.6	-29.1	- 1526	-20.4	- 5093.6	-30.3	- 400	-28.2
Waterbodies	1.2	5.1	1.2	0.30	2.4	3.9	1	0.1
Farmland	1747.4	15.3	- 1248	-19.3	499.4	4.0	-292	-4.3
Grassland	- 2197.6	-20.2	- 69.9	-23.8	-2267.5	21.5	- 100.1	-26.5
Total		100		100		100		100

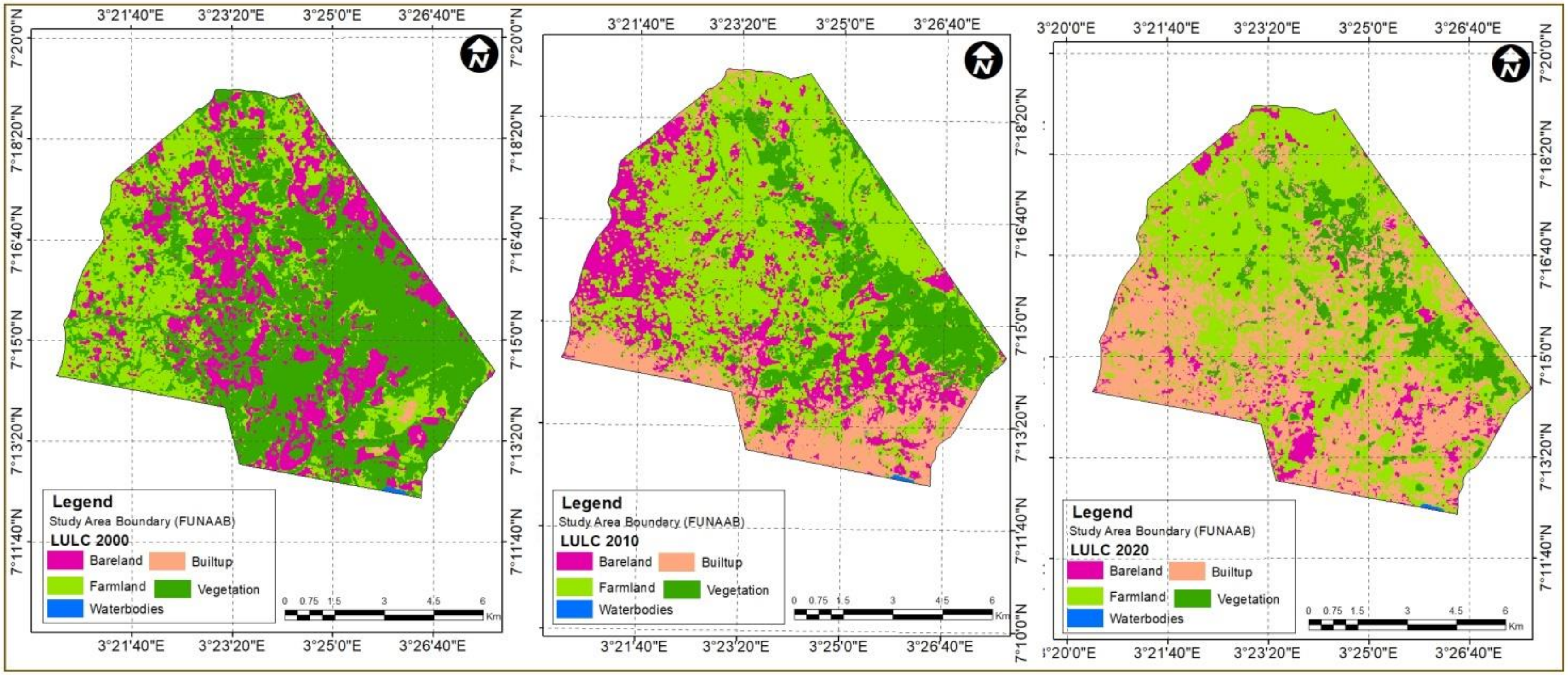

Figure 8: LULC (2000, 2010 and 2020) of the Federal University of Agriculture, Abeokuta

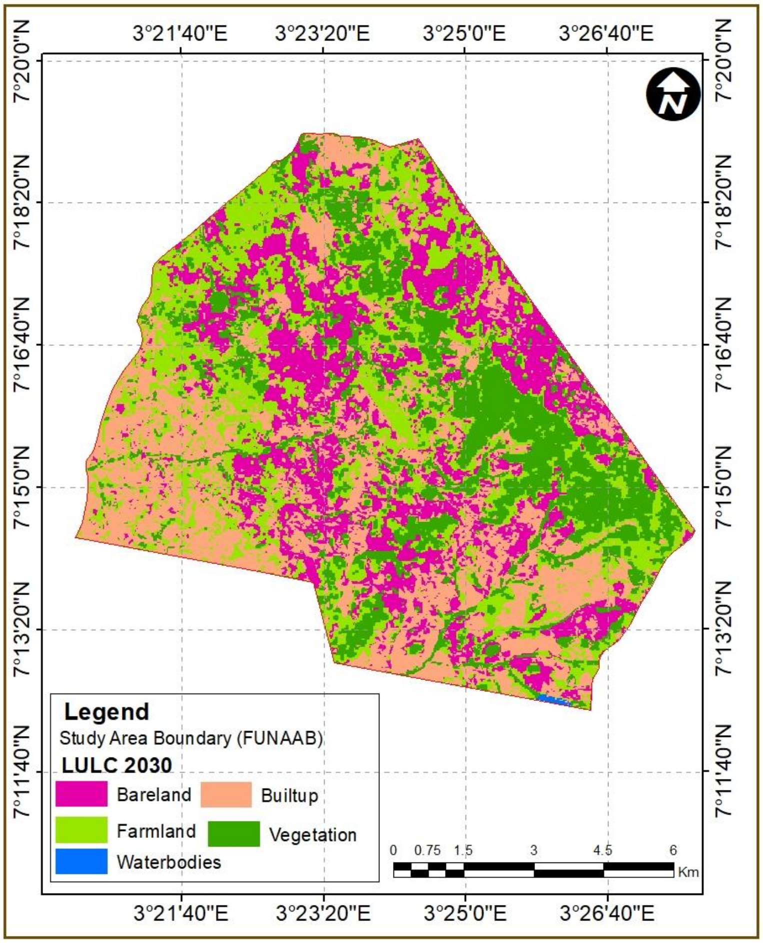

Figure 9: Modelled 2030 LULC of the Federal University of Agriculture, Abeokuta

Land suitability assessment for maize production

Soils, landform, climate and vegetation cover are essential in assessing land suitability (FAO, 2007b). Soil analysis, temperature (minimum and maximum), rainfall, Normalized difference vegetation index (NDVI), Soil adjusted vegetation index (SAVI), Land surface temperature (LST) and soil analysis were used to assess the suitability of the land for maize production of the studied area. The NDVI of the study area ranged in the following order 0.47 – 0.01 in the year 2000, 0.19 – 0.06 in the year 2010 and 0.09 – 0.06 in the year 2020 (See Fig. 4). Ahmed *et al.* (2016) opined that NDVI within the range of 0.25 – 0.26 can be classified as suitable for maize production when other land suitability criteria are suitable. It was also observed that the SAVI in the study area ranged from 0.19 – 0.06 in the year 2000, 0.47 – 0.01 in the year 2010 and 0.62 – 0.09 in the year 2020 (See Fig. 5). The result of the SAVI in tandem with the study carried out by Jiang *et al,* (2006) and highlighted that SAVI within the range of 0.08 – 0.38 can be termed adequate to support crop growth. The LST value in the study area ranged from 22 to 38 degrees Celsius (Fig. 6). According to Oluwatosin and Ogunkunle (1991); Jeevalakshmi *et al.* (2017) the LST within the ranged of 20 – 22 degree Celsius can be classified as highly suitable for rainfed maize production.

Soil properties and fertility status

The studied soil particle distribution varied from sandy clay loam to clay in texture. The pH value varied from 5.1 (strongly acidic) to 7.8 (slightly alkaline) in the studied soils. The acidic pH found in the studied soils could be due to effluent discharged into the studied soils especially, areas close to streams and rivers channels (Ufoegbune *et al.*, 2010). According to Amusan and Ashaye (1991) high rate of leaching of bases due to intense rainfall could be responsible for soils to be acidic in nature. Total nitrogen ranged from very low to medium (0.1 – 0.9%) and soil organic matter ranged from low to high (0.69 – 5.81%) in the studied soils. The low organic matter content could be attributed to continuous cropping without the addition of organic residue to the studied soils. Juo, *et al.*, (1994) and Akpan-Idiok, (2012) had earlier reported that continuous cropping of some soils in tropics could result into rapid decline in soil organic matter. This was equally the views and conclusions of previous studies, for example, Tobore *et al.*, (2021) and Senjobi and Ogunkunle (2010). The available phosphorus concentration obtained in this study fell between 0.2 – 3.4 mg kg^{-1} (very low). The available phosphorus concentration values were lower than the critical range (10 – 16 mg kg^{-1}) reported by Adeoye and Agboola, (1984) and Barber, (1984) soil interpretation guidelines. Findings also show that low soil pH could limit phosphorus availability to plants, which may cause deficiency symptoms of soil phosphorus even when they exist (USDA-NRCS, 1994). The exchangeable cations in the studied soils show that potassium ranged from very low to low (0.01 - 0.3 cmol/kg), calcium ranged from very low to very high (0.8 – 6.9 cmol/kg), magnesium also ranged from very low to moderate (0.7 – 2.7 cmol/kg), while sodium was found to be moderate in the studied area.

Principal component analysis of soil properties

The variable factor is presented in Figure (10). It was observed that variation among the soil properties i.e. Zinc (Zn) Total Nitrogen (TN), Organic Carbon (OC), Organic matter (OM), Phosphorus (P), and Potassium (K) exist in the same dimension (dimension 2). This simply means that as zinc decreases, TN, OC, OM, P, and K also decreases hitherto (Fig.10). Table 11 shows that the high R-square values were observed among O.C and N.

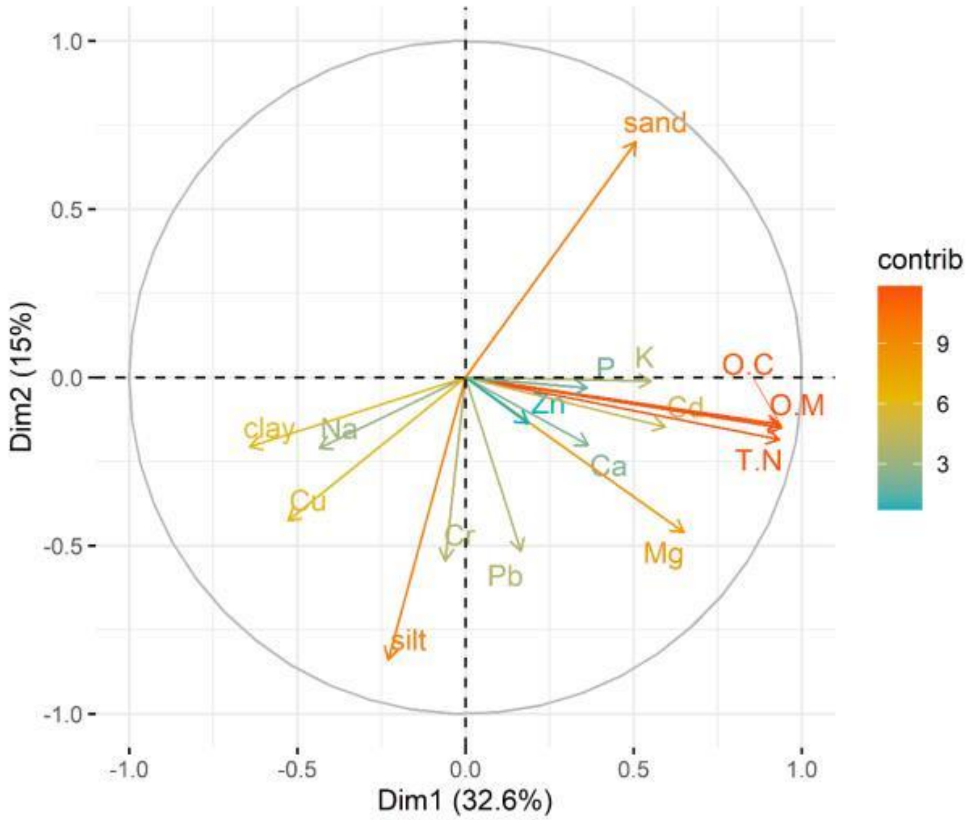

Figure 10: Variable factor map of Principal component analysis

Table 11: Correlation among the soil properties

	O.C	O.M	T.N	Na	Ca	Mg	K	Zn	Cu	Pb	Cr	Cd	P	Sand	Clay
O.M	**0.994**														
T.N	**0.988**	**0.996**													
Na	0.104	0.102	0.092												
Ca	0.081	0.081	0.084	0.003											
Mg	0.423	0.428	0.437	0.013	0.017										
K	0.190	0.193	0.204	0.093	0.010	0.105									
Zn	0.002	0.002	0.004	0.005	0.453	0.010	0.039								
Cu	0.160	0.147	0.126	0.204	0.044	0.034	0.153	0.004							
Pb	0.008	0.009	0.012	0.026	0.000	0.156	0.031	0.019	0.106						
Cr	0.000	0.000	0.003	0.020	0.176	0.005	0.001	0.008	0.162	0.035					
Cd	0.290	0.320	0.308	0.035	0.073	0.114	0.033	0.010	0.088	0.016	0.001				
P	0.150	0.124	0.116	0.066	0.000	0.036	0.022	0.031	0.027	0.006	0.006	0.000			
Sand	0.103	0.107	0.096	0.044	0.018	0.000	0.037	0.028	0.090	0.005	0.049	0.026	0.010		
Clay	0.229	0.245	0.244	0.012	0.038	0.134	0.056	0.084	0.059	0.064	0.009	0.065	0.008	0.549	
Silt	0.008	0.008	0.004	0.047	0.002	0.083	0.009	0.000	0.058	0.087	0.060	0.001	0.006	0.738	0.086

TN: Total Nitrogen; OM; Organic matter; Avail P: Available phosphorus; K: Potassium; Ca: Calcium; Mg: Magnesium; Na: Sodium; Zn: Zinc; Cu: Copper; Cr: Chromium; Cd: Cadmium.

Land suitability evaluation

The land suitability indices of the area show that the Rabia method was higher when compared to the Stories and Square root methods. The result of the Storie method revealed that maize suitability ranged from marginally not suitable (N1) to marginally suitable (S3); Square root method was dominantly marginally suitable (S3), while the Rabia method ranged from marginally suitable (S3) to highly suitable (S1) (Table 11). The major limiting factors for maize production in the studied area using the Stories and Square root methods are unevenly or low distribution of rainfall, slope and erosion hazard which are responsible for low soil nutrient level in the soils. The results of the parametric methods used in this study show that the Rabia method revealed area that are more suitable for optimum maize production. The Rabia method used in the study also in tandem with the study carried out by Khordebin and Landi (2011) who demonstrated that the Rabia method can assist to better revealed the real potentials or situations of land suitability for optimum crop production.

Table 12: Land suitability index and corresponding class for the three parametric methods (Storie, Square root and Rabia)

Units	FAO/UNESCO	Storie Method		Square Root Method		Rabia Method	
		Suitability index	Suitability class	Suitability index	Suitability class	Suitability class	Suitability class
1	Ferric Luvisols	60.2	S2	77.7	S1	80.5	S1
2	Ferric Lixisol	20.3	N1	45.4	S3	50.4	S2
3	Lithosols	20.1	N1	32.3	S3	39.8	S3
4	Ferric Cambisols	10.3	N1	32.7	S3	60.3	S2
5	Ferric Lixisol	20.8	N1	45.8	S3	55.9	S2
6	Gleyic Luvisols	30.3	S3	37.9	S3	49.3	S3
7	Ferric Luvisols	50.6	S2	40.6	S3	55.3	S2

Multicriteria assessment

The capability of GIS to analyze information across space and time has necessitated the increase and awareness in precision agriculture (Tobore *et al.*, 2019). Considering the criteria for land suitability assessment, the studied soils were found to range from (S1) highly, (S2), moderately (S3) marginally and (N1) marginally not suitable (Table 13). The integration of the AHP in MCE helped to show the spatial nutrient distribution of the soil nutrients and thus assisted in easy and adequate mapping of the land suitability of the studied area for maize production (Figure 11). The area with moderately (S2), marginally (S3) and marginally not suitable can be increased when properly managed through various soil management practices such as erosion control measure, etc. It was also observed that the appropriate use of the studied land for the purpose it is best suited for will increase the potential fertility of the studied soils. However, other studies supporting the present study can be found in Senjobi and Ogunkunle (2010) and Tobore et al., (2022).

Table 13: Suitability classes and area coverage for maize production

Classes	Suitability	Area	
		Ha	%
N2	Marginally not suitable	6915.4	69.1
S3	Marginally suitable	2598.5	26.0
S2	Moderately suitable	298.4	3.0
S1	Highly suitable	187.8	1.9
	Total	10,000	100

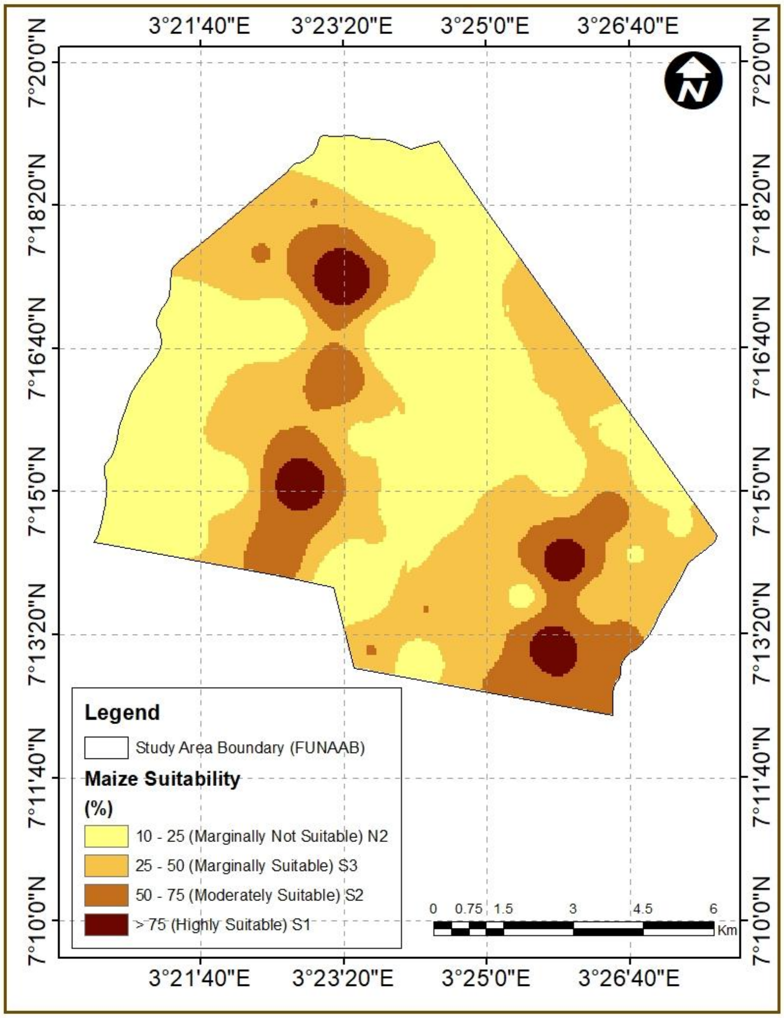

Figure 11: Map showing maize suitability of Federal University of Agriculture, Abeokuta

Conclusion

This study was aimed at modelling and simulating LULCCs and its impacts on land suitability at the Federal University of Agriculture Abeokuta, Ogun State, Nigeria. The integration of GIS and RS images serves as crucial tools in monitoring and mapping LULC change using the CA-Markov model. Based on the LULC analysis, it was discovered that the LULC change trends varied significantly from the year 2000 to 2030. The LULCCs revealed that the built-up areas and farmlands would increase by almost 86.99% and 7.07%, vegetation, grassland and waterbodies may decrease to 5.30%, 0.53% and 0.09% in the year 2030, respectively. This indicates that the area may continue to experienced gradual to sudden human activities such as deforestation. Thus, deforestation is known to be one of the main driving forces predicted for LULC change, especially in Nigeria. The land suitability criteria analysis used in this study made it easy and accurate in mapping the suitability of the studied soils for maize production. The soil suitability of the area showed that approximately 69.1% (6915.4 ha) of the area is determined as marginally not suitable (N2), whereas 26% (2598.5 ha) and 3.0% (298.4 ha) is described as marginally (S3) and moderately suitable (S2), respectively. The area that are highly suitable (S1) covered 1.9% (187.8 ha) of the studied area. Modelling and simulating the dynamics of LULC in this study will help to provide a basis for strategic planning, management and future decision-making by the policy makers. It is therefore recommended that the development of sustainable land-use practices needs to be improved to increase the suitability of the studied soils for optimum crop production such as maize. The present study demonstrated the efficiency of GIS and RS techniques in the area of land suitability assessment and LULC change analysis using the CA-Markov model and Rabia index method.

Acknowledgment

The author is sincerely grateful to the FUNAAB for their understanding and allowing us to carry out this study. We are equally thankful to the US Geological Survey (USGS) for assisting this research with data-sets.

Funding

This research did not receive any grant from any funding agent in the public, commercial or not-for-profit sectors.

REFERENCES

Adebekun, O. (1978). *Atlas of the Federal Republic of Nigeria*. 1st Ed., Under the Chairmanship of the National Atlas Committee, pp: 136.

Adeleye, N., Osabuohien, E. S., Adeogun, S., Fashola, S., Tasie, O., & Adeyemi, G. (2020). Access to land and food security: analysis of 'priority crops' production in Ogun State, Nigeria. In The palgrave handbook of agricultural and rural development in Africa (pp. 291–311). *Palgrave Macmillan*. doi: 10.1007/978-3-030-41513-6_14.

Adeoye, G.O., & Agboola, A. A. (1984). Critical levels of pH, available P, K, ZN and Mn and maize ear leaf content of P, Cu, and Mn in Sedimentary soil of Southeastern Niger. *Fertilizer Research* 6: 65 – 71.

Ahamed, T., Noguchi, R., Takigawa, T., & Tian, L. (2016). *Bioproduction engineering: Automation and precision agronomics for sustainable agricultural systems, (2nd ed.)*. Nova Science Publishers, Inc. New York, USA

Akpan-Idiok, A.U., (2012). Physiochemical properties, degradation rate and vulnerability potential of soils formed on coastal plain sands in Southeast, Nigeria. *International Journal of Agricultural Research*.

Alemayehu, F., Taha, N., Nyssen, J., Girma, A., Zenebe, A., Behailua, M., Deckers, S., & Poesen, J. (2009). The impacts of watershed management on land use and land cover dynamics in Eastern Tigray (Ethiopia). *Resources, Conservation and Recycling*, 53:192-198.

Amusan, A. A. & Ashaye, T. I. (1991). Granitic-gneiss derived soils in humid forest tropical southwestern Nigeria: Genesis and classification. *Ife Journal of Agriculture*, 13 (1& 2): 1 – 20.

Anderson, J. R., Hardy, J. T. R., & Witmer, R. E., (1976). A land use and land cover classification A. *Pensuk and RP Shrestha/GMSARN International Journal*, 2 (2008), 190.

Anderson, J. M., & Ingram, J. S. L. (1993). *Tropical soil biology and fertility: handbook of Method of Analysis*. UK:International Wallingford, (pp. 38–39).

Ansari, A., Sadough, M. B., & Shamse, B. (2008a). *Ecological investigation of thecommon crane Grus in Mighan Wetland, 3*. Podoces: Markazi Province, Central Iran

Bakx, T. R. M., Koma, Z., Seijmonsbergen, A. C. & Kissling, W. D. (2019). Use and categorisation of LiDAR vegetation metrics in avian diversity and species distribution research. Dryad Digital Repository. https://doi.org/10.5061/dryad.tm28hb6.

Balogun, I., & Ishola, K. (2017). Projection of future changes in landuse/landcover using cellular automata/markov model over Akure city, Nigeria. *Journal of Remote Sensing Technology*. 5 (1), 22–31.

Barber, S. A. (1984). *Soil nutrient bioavailabilty, a mechanistic approach*. New York: Willey.

Biro, K., Pradhan, B., Buchroithner, M. and Makeschin, F. (2013). Land use/Land cover change analysis and its impact on soil properties in the northern part of Gadarif region, Sudan, *Land Degradation and Development*, 24, 90–102. https://doi.org/10.1002/ldr.1116.

Bouyoucos, G. H. (1962). Hydrometer method for making particle size analysis of soils. *Agronomy Journal*, 54, 464 –465. https://doi.org/10.2134/agronj1962.00021962005400050028x.

Cohen, B. (2006). Urbanization in developing countries: Current trends, future projections, and key challenges for sustainability. *Technology in Society*, 28(1–2), pp. 63–80 http://dx.doi.org/10.1016/j.techsoc.205.10.005.

Das, S. & Ting Y. (2017). Evaluation of wet digestion methods for quantification of metal content in electronic scrap materials. *Resources* 64.

d'Entremont, R.P. & Thomason, L.W. (1987). Interpreting meteorological satellite images using a color-composite technique. Bull. Am. Meteorol. Soc. 68 (7), 762–768.

Ekanade, O. (2007). Cultured Trees, their Environment and our Legacies. Inaugural Lecture Series 198. University Press Ltd., Obafemi Awolowo, pp: 44

Epule, T. E., Ford, J. D., Lwasa, S., & Lepage, L., (2017) .Vulnerability of maize yields to droughts in Uganda. Water (Switzerland). https://doi.org/10.3390/w9030181FAO/IUSS Working Group, 2006. A framework for land evaluation. Rome: Soils Bulletin 31, pp 25-42.

Federal Office of Statistics, (1988). Annual Abstracts of Statistics. 1988 Edn., Federal Office of Statistics, Lagos, Nigeria, pp: 218.

FAO, (1976). Soil and Terrain Database for North and Central Eurassia (Version 1.0), FAO, ROME.

FAO., (1990). *Agro-Ecological Zoning, Guidelines*. Food and Agricultural Organization of the United Nations, Rome.

FAO, Rome., (2007a). *The State of Food Insecurity in the World.* Food and Agriculture Organization of the United Nations, Rome.

FAO., (2007b). *Land Evaluation, towards a revised framework.* FAO, Rome, Italy

FAO., (2009). Landcover Classification System: Classification Concepts and user Manual Software Version 2. Food and Agriculture Organisation, Rome, Italy, pp: 190.

FAO., (2010). Global Forest Resources Assessment 2010 - Main report. FAO Forestry Paper. Retrieved from Rome, Italy.

Foody, G.M., (2002). Status of land cover classification accuracy assessment. *Remote Sens. Environ*. 80 (1), 185–201.

Foley, JA, Costa, MH., Delire, C., Ramankutty, N., & Snyder, P., (2005). Green surprise? How terrestrial ecosystems could afect earth's climate. *Front Ecol Environ* 1(1):38–44

Gao, Y., & Mas, J. F., (2008). A Comparison of the Performance of Pixel Based and Object Based Classifications over Images with Various Spatial Resolutions. Online Journal of Earth Sciences, 2(1), 27–35.

Gilabert, M. A., González-Piqueras, J., García-Haro, F. J., & Meliá J., (2002). A generalized soil-adjusted vegetation index," *Remote Sens. Environ.* 82, 303-310. [doi:10.1016/S0034-4257(02)00048-2

Gilbert, D.A.E., (1969). A Map Book of West Africa Metric Edition. Macmillan Education Ltd., London and Basingstoke, pp: 66.

Gong, W., Yuan, L., Fan, W., & Stot, P., (2015). Analysis and simulation of land use spatial patern in Harbin prefecture based on trajectories and celular automata, Markov modelling. Int. J. Apl. Earth Obs., 34: 207-216

Hasan, S.S., Deng, X., Li, Z., & Chen, D., (2017). Projections of Future Land Use in Bangladesh under the Background of Baseline, Ecological Protection and Economic Development. *Sustainability* 9, 505. http://doi:10.3390/su9040505.

Huete, A. R., (1988). A soil-adjusted vegetation index (SAVI). Remote Sens. Environ. 25:295-309.

Hussain, S. (2018). Land use/land cover classification by using satellite NDVI tool for sustainable water and climate change in Southern Punjab. COMSATS Univ. Islamabad. MS thesis. https://doi.org/10.13140/RG.2.2.32363.69923 .

IITA, (1988). Selected Methods for Soil and Plant Analysis. Manual series No. 1 Ibadan Nigeria

Jesus, J. B., & Santana, I. D. M., (2017). Estimation of land surface temperature in caatinga area using Landsat 8 data, 7, 150–157. Retrieved from https://periodicos.ufpe.br/revistas/jhrs/article/view/22766.

Jeevalakshmi, D., Narayana Reddy, S., & Manikiam, B., (2017). Land surface temperature retrieval from LANDSAT data using emissivity estimation. International Journal of Applied Engineering Research, 12(20), 9679–9687.

Jiang, Z., Huete, A. R., Chen, J., Chen, Y., Li, J., & Yan, G., (2006). Analysis of NDVI and scaled difference vegetation index retrievals of vegetation fraction. Remote Sensing of Environment, 101(3), 366–378. https://doi.org/10.1016/j.rse.2006.01.003.

Juo, A.S.R., Caldwell, J., & Kang, B.T., (1994). Place of alley cropping in sustainable agriculture in the tropics. Transaction of the 15th International Soil Science Congress 7: 98 – 109.

Khordebin S A., Landi, (2011). Comparison of the Land Qualitative Suitability with the Use of FAO Method and Ales Model for Major Crops in Sardasht of Behbahan Khuzestan Province, Iran," Middle-East Journal of Scientific Research vol. 10, no. 4, pp. 477-481.

Lambin, E.F., (1999). Are agricultural land-use models able to predict changes in land-use intensity. Agriculture, Ecosystems & Environment 82(1-3):321-331.

Lambin, E. F., Geist, H. J., & Lepers, E., (2003). Dynamics of land-use and land-cover change in tropical regions. Annual Review of Environment and Resources, 28(1), 205–241

Lepers, E., Lambin, E F., Janetos, A C., DeFries, R., Achard, F., Ramankutty, N., & Scholes, R J., (2005). A synthesis of information on rapid land-cover change for the period 1981–2000. *Bioscience*.;55:115–24. doi:10.1641/0006-3568(2005)055[0115:ASOIOR]2.0.CO;2.

Li, L., Zhao, J., & Yuan, T., (2004). Study on approaches of land suitability evaluation for crop production using GIS. IFIP Advances in Information and Communication Technology. IFIP AICT 345, pp. 587–596. https://doi.org/10.1007/978- 3-642-18336-2_72.

Liu, H., (2005). Accuracy analysis of remote sensing change detection by rule-based rationality evaluation with post-classification comparison. International Journal of Remote Sensing, 25(5), 1037–1050. http://dx.doi.org/10.1080/0143116031000150004

Lu, D., Mausel, P., Brondizio, E., & Moran, E., (2004). Change detection techniques. International Journal of Remote Sensing, 25(12), 2365–2401.

Ma, X., Zuo, H., Tian, M., Zhang, L., Meng, J., Zhou, X., Min, N., & Chang, X., Liu, Y., (2012). Assessment of heavy metals contamination in sediments from three adjacent regions of the Yellow River using metal chemical fractions and multivariate analysis techniques.

McLean, E. O., Dumford, S. W. F., & Coronel, S. W., (1982). A comparison of several methods of determining lime requirements of soil. Soil Science Society of America Proceedings, 30, 26

Mishra, V.N., Rai, P.K., Prasad, R., Punia, M., & Nistor, M.M., (2018). Prediction of spatio-temporal land use/land cover dynamics in rapidly developing Varanasi district of Uttar Pradesh, India, using geospatial approach: a comparison of hybrid models. Applied Geomatics 10 (3), 257–276.

Mustafa, A. A., Singh, M., Sahoo, R. N., Ahmed, N., Khanna, M., Sarangi, A., & Mishra, A. K., (2011). Land suitability analysis for different crops: a multi criteria decision making approach using remote sensing and GIS. Researcher.3: 1-84.

Mwavu and Witkowski,, (2008). Population structure and regeneration of multiple use tree species in a semi deciduous African tropical rainforest implications for primary conservation.

Nelson, D. W., & Sommers, L. E., (1996). Total carbon, organic carbon, and organic matter. In D.L. *Sparke (Ed.), Methods of soil analysis. Part3. Chemical methods* SSSA book seriesno. 5 (pp. 961–1010). Madison: ASA and SSSA.

Oluwatosin, G. A., & Ogunkunle, A. O., (1991). Suitability rating of some soils of the savanna zone of South-western Nigeria for rainfed Maize. Nigeria Journal of Soil Science 10: 1-24.

Pontius Jr, R.G., & Millones, M., (2011). Death to Kappa: birth of quantity disagreement and allocation disagreement for accuracy assessment. *Int. J. Rem. Sens*. 32 (15), 4407–4429.

Rabia, A. H., (2012). “A GIS based land suitability assessment for agricultural planning in Kilte Awulaelo district, Ethiopia,” The 4th International

Congress of ECSSS, EUROSOIL 2012 "soil science for the benefit of mankind and environment", Bari, Italy, pp. 1257, 2-6 June

Rasul, A., H., Balzter, C., & Smith, (2015). Spatial Variation of the Daytime Surface Urban Cool Island during the Dry Season in Erbil, Iraqi Kurdistan, from Landsat 8." *Urban Climate* 14: 176–186.doi:10.1016/j.uclim.2015.09.001

Smyth, A .J. & Montgomery R.F., (1962). *Soils and Landuse in Central Western Nigeria*. The Government Printer, Ibadan, Western Nigeria, pp: 265.

Saaty, T. L., (1977). A scaling method for priorities in hierarchical structures," J Math Psychol, vol. 15, pp. 234–281. 1977.

Saaty, T. L., & Vargas L. G., (2001). "Models, methods, concepts, and applications of the analytic hierarchy process," Boston etc., Kluwer Academic, pp. 327,

Senjobi, B. A., (2007). Comparative assessment of the effect of land type and land use type on land degradation and soil degradation in Ogun state Nigeria. *Phd Thesis,. Department of Agronomy, University of Ibadan Oyo State Nigeria* , 261.

Senjobi, B.A., & Ogunkunle, O A., 2010. Effect of Land Use on Soil Degradation and Soil Prodcutivity Decline on Alfisols and Ultisols in Ogun State in Southern Western Nigeria. *J. Agric. Conspectus Sci*. Faculty of Agriculture, University of Zagreb, Crotia, 75(1): 9-19.

Singh, P, Gupta, P., & Singh, M., (2014). Hydrological inferences from watershed analysis for water resource management using remote sensing and GIS techniques. *Egypt J Remote Sensing Space Sci* 17:111–121.

Subedi, P., & Thapa, B., (2013). Aplication of a Hybrid Cellular Automaton–Markov (CA-Markov) Model in land use change prediction: A case study of Sadle Crek Drainage Basin, Florida. *Apl. Ecol. Environ. S*, 1(6): 126-132.

Su, C., Jiang, L., & Zhang, W., (2012). A review on heavy metal contamination in the soil worldwide: Situation, impact and remediation techniques. *Environmental Skeptics and Critics*., 3(2), 24–38. https://doi.org/10.1016/j.envint.2014.04.014.

Sun, Y., Zhou, Q., Xie, X., & Liu, R., (2013). Spatial, sources and risk assessment of heavy metal contamination of urban soils in typical regions of Shenyang, China. *Journal of Hazardous Materials*. 174(1–3), 455–462 https://doi.org/10.1016/j.jhazmat.2009.09.074.

Sotona, T, Salako, F., & Adesodun, J., (2014). Soil physical properties of selected soil series in relation to compaction and erosion on farmers' fields at Abeokuta, southwestern Nigeria. *Archives of Agronomy and Soil Science*, 60:6, 841-857, DOI: 10.1080/03650340.2013.844334

Story, M., & Congalton, R.G., (1986). Accuracy assessment: a user's perspective. Photogramm. Eng. Rem. Sens. 52 (3), 397–399.

Sys, I. E., Van Ranst, J., Debaveye, 1991. *Land evaluation, part I. Principles in land evaluation and crop production calculations.* General administration for development cooperation, Brussels, pp. 40-80.

Tobore, A.O., Alabi, K.A., Ogundiyi., T.O., & Samuel, B., (2019). Digital mapping of cultivated land in two peri-urban areas of Ibadan, Nigeria. *Nigeria Journal of Soil Science*.

Tobore, A. O, Adedeji, O. H. Senjobi, B. A, & Sodiq, O. **(**2021) Geospatial Suitability Assessment of Wetland Soils for Rice Production in Federal University of Agriculture Abeokuta, Ogun State, Nigeria. *Discovery Agriculture*, 7(17): 1 – 25. Publisher: Discovery scientific society.

Tobore, A., Senjobi, B., Ogundiyi, T., & Bamidele, S. (2021). Geospatial assessment of wetland soils for rice production in Ajibode using geospatial techniques. *Open Geosciences*, 13(1), 310–320. https://doi.org/10.1515/geo-2020-0227

Tobore, A.O., Senjobi, B.A., Oyerinde, G.T., & Samuel, B., (2022) .Geospatial Soil Suitability Assessment for Maize (Zea mays) Production in Derived Savanna of Agricultural Research and Training, OYO State, Nigeria. *Jordan Journal of Earth and Environmental Science* JJEES 14 (1). 9 – 18. ISSN 1995 -6682.

Tobore, A. O, Nkwunonwo, U.C. & Senjobi, B. A. (2022). Combined remote sensing and multi-criteria analysis of wetland soil potential for rice production: case study of Ogun river basin. *Nigeria, African Geographical Review*, DOI: 10.1080/19376812.2022.2104736

Ufoegbune, G.C., Oyedepo, J.A., Awomeso, A., & Eruola, O., (2010). "Spatial Analysis of Municipal Water Supply in Abeokuta Metropolis, South Western Nigeria". REAL CORP 2010 Proceedings. Tagungsband: Vienna, Austria. 18- 20 May 2010. http://www.corp.at. M. Schrenk, V. Vasily, P. Popovich, and P. Zeile (eds.)

Udo, E. J., Ibia, T. O., Ogunwale, J. A., Ano, A. O., & Esu, I. E., 2009. *Manual of soil, plant and water analyses*. 539 Lagos: Sibon Books Ltd 183 pp.

USDA-NRCS. (1994). *Inherent factors affecting soil phosphorus*.

Victorino, T.J., (2011). "Guinean Forest-Savanna Mosaic Log Press: Science. 30 Oct 2011:104.

Vargahan, B., Shahbazi, F., & Hajrasouli, M., (2011). "Quantitative And Qualitative Land Suitability Evaluation For Maize Cultivation In Ghobadlou Region, Iran," *Ozean Journal Of Applied Science*s, vol. 4, no. 1, Issn 1943-2429.

Verburg, P.H., Soepboer, W., Limpiada, R., Espaldon, M.,& Sharifa, M., (2002). Land use change modelling at the regional scale: The CLUE-S model. *Environmental Management*, 30(3), 391–405. doi:10.1007/s00267-002-2630-x

Verheye, W., (2008). LAND EVALUATION. *In Land use and Land Cover (II). UNESCO-EOLSS*, Belgium: Ghent University Library.

Walkley, A., & Black, I. A., (1939). An examination of Degtjareff method for determining soil organic matter and a proposed modification of the chromic acid titration method. *Soil Science*, 37, 29 – 38. https://doi.org/10.1097/00010694193401000-00003.

Wu, C.D., Cheng, C.C., Lo, H.C., & Chen Y.K., (2013). Application of SEBAL and Markov Models for Future Stream Flow Simulation Through Remote Sensing. *Water Resource Management.* 24(14):3773–97. https://doi. org/10.1007/s11269-010-9633-9.

Zhang, H., Jin, X., Wang, L., Zhou, Y., & Shu, B., (2015). Multi-agent based modelling of spatiotemporal dynamical urban growth in developing countries: simulating future scenarios of Lianyungang city, China. Stoch. Environ. Res. Risk A, 29(1): 63-78.

Zheng, J., Niu, J., Bao, T., Buyantuyev, A., Zhang, Q., Dong, J., & Zhang, X., (2015). Human induced dry-land degradation in Ordos plateau, China, revealed by multi-level statistical modelling of normalized difference vegetation index and rainfall time series. *J. Arid Land*, 6, 219–229, https://doi.org/10.1007/s40333-0130203-x

Zubair, A.O., (2006). Change detection in land use and land cover Using remote sensing data and GIS: A case study of Ilorin and its environs in Kwara State. *Unpublished (Master's thesis), University of Ibadan*.